Evidence that the tandem-pleckstrin-homology-domain-containing protein TAPP1 interacts with Ptd(3,4)P_2 and the multi-PDZ-domain-containing protein MUPP1 *in vivo*

Wendy A. KIMBER*[1], Laura TRINKLE-MULCAHY‡, Peter C. F. CHEUNG*, Maria DEAK*, Louisa J. MARSDEN*, Agnieszka KIELOCH†, Stephen WATT‡, Ronald T. JAVIER§, Alex GRAY†, C. Peter DOWNES†, John M. LUCOCQ‡ and Dario R. ALESSI*

*MRC Protein Phosphorylation Unit, MSI/WTB Complex, University of Dundee, Dow Street, Dundee DD1 5EH, Scotland, U.K., †Division of Signal Transduction Therapy, MSI/WTB Complex, University of Dundee, Dow Street, Dundee DD1 5EH, Scotland, U.K., ‡School of Life Sciences, MSI/WTB Complex, University of Dundee, Dow Street, Dundee DD1 5EH, Scotland, U.K., and §Department of Molecular Virology and Microbiology, Baylor College of Medicine, Houston, TX 77030, U.S.A.

PtdIns(3,4,5)P_3 is an established second messenger of growth-factor and insulin-induced signalling pathways. There is increasing evidence that one of the immediate breakdown products of PtdIns(3,4,5)P_3, namely PtdIns(3,4)P_2, whose levels are elevated by numerous extracellular agonists, might also function as a signalling molecule. Recently, we identified two related pleckstrin-homology (PH)-domain-containing proteins, termed 'tandem-PH-domain-containing protein-1' (TAPP1) and TAPP2, which interacted *in vitro* with high affinity with PtdIns(3,4)P_2, but did not bind PtdIns(3,4,5)P_3 or other phosphoinositides. In the present study we demonstrate that stimulation of Swiss 3T3 or 293 cells with agonists that stimulate PtdIns(3,4)P_2 production results in the marked translocation of TAPP1 to the plasma membrane. This recruitment is dependent on a functional PtdIns(3,4)P_2-binding PH domain and is inhibited by wortmannin, a phosphoinositide 3-kinase inhibitor that prevents PtdIns(3,4)P_2 generation. A search for proteins that interact with TAPP1 identified the multi-PDZ-containing protein termed 'MUPP1', a protein possessing 13 PDZ domains and no other known modular or catalytic domains [PDZ is postsynaptic density protein (**PSD**-95)/*Drosophila* disc large tumour suppressor (**d**lg)/tight junction protein (**Z**O1)]. We demonstrate that immunoprecipitation of endogenously expressed TAPP1 from 293-cell lysates results in the co-immunoprecipitation of endogenous MUPP1, indicating that these proteins are likely to interact with each other physiologically. We show that TAPP1 and TAPP2 interact with the 10th and 13th PDZ domain of MUPP1 through their C-terminal amino acids. The results of the present study suggest that TAPP1 and TAPP2 could function in cells as adapter proteins to recruit MUPP1, or other proteins that they may interact with, to the plasma membrane in response to signals that elevate PtdIns(3,4)P_2.

Key words: adapter protein, oxidative stress, phosphoinositide, phosphoinositide 3-kinase, scaffolding protein.

INTRODUCTION

Agonists, including growth factors, hormones and cytokines, induce the activation of members of the phosphoinositide 3-kinase (PI 3-kinase) group of lipid kinases, which phosphorylate PtdIns(4,5)P_2 at the D3 position of the inositol head group to generate PtdIns(3,4,5)P_3 [1]. This lipid is located at the plasma membrane and functions as an important cellular 'second messenger', triggering the activation of a network of signalling pathways that regulate many physiological events, including cell survival and responses to insulin. A key mechanism by which PtdIns(3,4,5)P_3 is known to activate downstream signal-transduction events is by its ability to interact specifically with members of a group of proteins that possess a certain type of pleckstrin-homology (PH) domain [2]. This interaction results in their recruitment to the plasma membrane, where they are brought into the vicinity of their physiological effectors and/or are activated by phosphorylation at this location (reviewed in [1,3]).

PtdIns(3,4,5)P_3 can be further metabolized to PtdIns(3,4)P_2 through the action of 5-phosphatases termed Src-homology-domain-2-containing inositol 5-phosphatase-1 (SHIP1) and SHIP2 [4,5]. Several, but not all PH-domain-containing proteins that interact with PtdIns(3,4,5)P_3, also bind to PtdIns(3,4)P_2 with similar affinity. These include the PH domains of protein kinase B (PKB, also known as Akt) [6], 3-phosphoinositide-dependent protein kinase-1 (PDK1) [7,8] and the **d**ual **a**daptor for **p**hosphotyrosine and **p**hosphoinositides-1 (DAPP1) [9–11]. Recent work has suggested that PtdIns(3,4)P_2 can also be generated via a pathway involving the phosphorylation of PtdIns3P by an as-yet-uncharacterized PI 4-kinase in response to cross-linking of platelet integrin receptors [12,13]. It has also been shown that treatment of several cell lines with H_2O_2 resulted in a large

increase in PtdIns(3,4)P_2 levels, with only a small and transient increase in PtdIns(3,4,5)P_3 [14]. The pathway by which PtdIns(3,4)P_2 is generated in response to H_2O_2 has not been characterized.

These findings raise the possibility that PtdIns(3,4)P_2 functions as a signalling lipid *in vivo*. Thus far only two related proteins of unknown physiological function, termed the **ta**ndem-**PH**-domain-containing **p**rotein-**1** (TAPP1) and TAPP2, have been identified, which possess the ability to bind PtdIns(3,4)P_2 specifically. TAPP1 and TAPP2 consist of two sequential PH domains, of which the C-terminal one binds to PtdIns(3,4)P_2 with high affinity. In our hands the C-terminal PH domain of TAPP1 does not interact significantly with PtdIns(3,4,5)P_3 or any other phosphoinositide that has been tested [15]. The three-dimensional structure of the C-terminal PH domain of TAPP1 has recently been determined, establishing the mechanism by which it interacts specifically with PtdIns(3,4)P_2 [16]. It should be noted, however, that Lemmon and colleagues [11] have reported that the C-terminal PH domain of TAPP1 interacts weakly with Ins(1,3,4,5)P_4, the water-soluble head group of PtdIns(3,4,5)P_3, raising the possibility that, *in vivo*, TAPP1 could potentially bind Ins(1,3,4,5)P_4 or PtdIns(3,4,5)P_3. In the present study we provide evidence that TAPP1 interacts specifically with PtdIns(3,4)P_2 *in vivo*, resulting in its recruitment to the plasma membrane. Furthermore, we show that TAPP1 and TAPP2 interact through their C-terminal residues with a multi-PDZ-containing protein termed MUPP1 [17].

MATERIALS AND METHODS

Materials

Protease-inhibitor-cocktail tablets, FuGENE™ 6 transfection reagent and G418 (Geneticin) were from Roche, insulin-like growth factor-1 (IGF1) and microcystin-LR (a cyanobacterial peptide toxin) were from Life Technologies, foetal bovine serum and other tissue-culture reagents were from BioWhittaker, dimethyl pimelimidate and H_2O_2 were from Sigma, and platelet-derived growth factor (PDGF)-BB was from Calbiochem. The precast 4–12%-(w/v)-polyacrylamide/SDS/Bis-Tris gradient gels were from Invitrogen.

Antibodies

Antibodies recognizing TAPP1 were raised in sheep against the whole TAPP1 protein expressed in *Escherichia coli* as a glutathione S-transferase (GST) fusion. The antibodies recognizing MUPP1 were raised against a C-terminal fragment of MUPP1 comprising residues 926–1676 expressed in *E. coli* as a GST-fusion protein and are available from Upstate Biotechnology. The anti-LKB1 antibody used as a negative control was raised against the whole LKB1 (a serine/threonine kinase) protein [18]. The antibodies were affinity-purified on CH-Sepharose covalently coupled to the protein antigens used to raise the antibodies. The anti-TAPP1 and anti-MUPP1 antibodies were then passed through a column of CH-Sepharose coupled to GST and the antibody that did not bind was selected. Secondary antibodies coupled to horseradish peroxidase used for immunoblotting were from Pierce, monoclonal antibodies recognizing GST and Flag epitope tags were from Sigma.

General methods and buffers

Restriction-enzyme digests, DNA ligations, site-directed mutagenesis and other recombinant-DNA procedures were performed using standard protocols. All DNA constructs were verified by

DNA sequencing. This was performed by The Sequencing Service, School of Life Sciences, University of Dundee, Dundee, Scotland, U.K., using DYEnamic ET terminator chemistry (Amersham Pharmacia Biotech) on Applied Biosystems automated DNA sequencers. Buffer A contained 50 mM Tris/HCl, pH 7.5, 0.1 mM EGTA, 0.27 M sucrose and 0.1% (v/v) 2-mercaptoethanol. Buffer B contained 50 mM Tris/HCl, pH 7.5, and 0.1 mM EGTA. Buffer C contained 50 mM Tris/HCl, pH 7.5, 1 mM EGTA, 1 mM EDTA, 1% (w/w) Triton X-100, 1 mM Na_3VO_4, 50 mM NaF, 5 mM sodium pyrophosphate ($Na_2H_2P_2O_7$), 0.27 M sucrose, 1 μM microcystin-LR, 0.1% (v/v) 2-mercaptoethanol and 'complete' proteinase-inhibitor cocktail (one tablet/25 ml). Sample Buffer contained 50 mM Tris/HCl, pH 6.8, 2% (w/w) SDS, 10% (v/v) glycerol and 1% (v/v) 2-mercaptoethanol.

DNA constructs

Mammalian fusions GST–TAPP1 and GST–TAPP2 in the pEBG-2T expression vector have been described previously [15]. The FLAG-epitope-tagged full-length human TAPP1 was amplified by PCR using the primers N1 (5′-GGATCCGCCACCATG-GACTACAAGGACGACGATGACAAGATGCCTTATG-TGGATCGTCAGAATCGC-3′) and N2 (5′-GGATCCAA-GAGTACACCTAAGAGGCAGTATAATATA-3), with the TAPP1 pEBG2T vector as the template. FLAG-epitope-tagged TAPP1$_{CT}$ was amplified using the primers N1 and N3 (5-GGATCCTCACGGAAGGCTCGCATCGTCCAAGTCT-3′), that truncate the last four amino acids of TAPP1. Full-length FLAG-epitope-tagged mouse TAPP2 was amplified with the primers N4 (5′-GGATCCGCCACCATGGACTACAAGGAC-GACGATGACAAGATGCCTTATGTGGATCGGCAGAA-CCGA-3′) and N5 (5′-GGATCCTCACACATCAGAGGTT-CGTATGTTTTCGTC-3′). Mouse TAPP2-ΔCT lacking the four C-terminal amino acids was amplified with primers N4 and N6 (GGATCTCATCGTATGTTTTCGTCATCAAGGTTGAA-TAC). The resulting PCR fragments were ligated into the pCR2.1-Topo vector (Invitrogen) and the sequences were verified. *Bam*H1–*Bam*H1 insert fragments from this intermediate vector were subcloned into the pEBG-2T expression vector. The Myc–TAPP1[R28L] and Myc–TAPP1[R211L] mutants in the pEBG-2T vector were generated by subcloning *Bam*H1–*Bam*H1 fragments of these cDNAs from pGEX-4T expression vector described previously [15] into the *Bam*H1 site of pEBG-2T. *Bam*H1–*Bam*H1 fragments of FLAG–TAPP1, Myc–TAPP1-[R28L], Myc–TAPP1[R211L] and FLAG–TAPP1$_{CT}$ were cloned into the *Bgl*II site of the pEYFP-C1 vector (YFP is yellow fluorescent protein). *Bam*H1–*Bam*H1 fragments of TAPP1$_{CT}$ encoding residues 182–304 of human TAPP1 was derived from a pGEX-4T expression vector [16] and cloned into the *Bgl*II site of the pEYFP-C1 vector. The FLAG-tagged and general receptor for phosphoinositides-1 (GRP1) PH domain from amino acids 211–400 in the pEBG2T vector [15] was subcloned into the *Bgl*II site of pEYFP-C1 as a *Bam*H1–*Bam*H1 fragment. Wild-type TAPP1 and TAPP2 or mutant TAPP1$_{CT}$ and TAPP2$_{CT}$ were subcloned into the *Eco*R1 site of pAS2-1 vector as *Eco*R1–*Eco*R1 fragments derived from pCR2.1-Topo. To create a bacterial GST expression vector comprising residues 926–1676 of human MUPP1, which was employed to raise the MUPP1 antibody employed in the present study, the *Eco*R1–*Xho*1 fragments of a pACT2 that was isolated in the TAPP1 two-hybrid clone was subcloned into the same sites of pGEX-4T-2. Other GST bacterial constructs encoding different PDZ domains of mouse GST–MUPP1 employed in the studies described in Figure 6 (below) were described previously [19]. To generate the mammalian

GST-tagged MUPP1 fragments employed in the experiments described in Figure 5 (below), *Bgl*II–*Bgl*II fragments derived from pACT2 TAPP1 interacting two-hybrid clones were sub-cloned into the *Bam*H1 site of pEBG-3X vector. The constructs of MUPP1$_{11-13}$ fragment comprise amino acids 1689–2042 and those of the MUPP1$_{13}$ fragment comprise amino acids 1885–2042. The MUPP1$_{11-12}$ fragment, comprising amino acids 1689–1924, was generated by introducing a STOP mutation in the MUPP1$_{11-13}$ pEBG2T construct.

Cell culture, stimulation and cell lysis

Mouse fibroblast Swiss 3T3 and human embryonic kidney 293 cells were cultured on 10 cm-diameter dishes in Dulbecco's modified Eagle's medium supplemented with 10 % (v/v) foetal-calf serum. Where indicated the cells were cultured in the absence of serum. Wortmannin was dissolved in DMSO at a 1000-fold higher concentration than that at which it was used. It, or the equivalent volume of DMSO as a control, was added to the tissue-culture medium 10 min prior to stimulation. The cells were stimulated with the indicated agonists and either fixed in 4 % (v/v) paraformaldehyde or lysed in 1 ml of ice-cold Buffer C. In the latter case the lysates were centrifuged at 4 °C for 5 min at 16000 *g*. The supernatants were frozen in liquid nitrogen and stored at −80 °C. Protein concentrations were determined using the Bradford method, and BSA was employed as the standard.

Generation of stable Swiss 3T3 cell lines expressing YFP and YFP–TAPP1$_{CT}$

Swiss 3T3 cells were cultured to 50 % confluence on 10 cm-diameter dishes and transfected with 2.5 μg of the pEYFP–TAPP1$_{CT}$ or empty pEYFP vector using FuGENE™ 6 transfection reagent following the manufacturer's (Roche) protocol. A triplicate set of dishes was used for each condition. After 48 h, G418 was added to the medium to a final concentration of 3 mg/ml, and the medium was changed every 48 h, maintaining G418. After 10 days, colonies of fluorescing cells were isolated and expanded. We selected a cell line for analysis that expressed an intermediate level of YFP or YFP–TAPP1$_{CT}$.

Microscopy and image analysis

In experiments in which the cells were fixed prior to analysis, the cells were grown on coverslips (no. 1$\frac{1}{2}$) and after stimulation were washed in PBS and fixed for 10 min in freshly prepared 4 % (v/v) paraformaldehyde in PHEM Buffer (60 mM Pipes, 25 mM Hepes, 10 mM EGTA and 2 mM MgSO$_4$, pH 7.0). The cells were washed twice with PBS and mounted on to slides using Mowiol. For live-cell imaging the cells were grown on 42 mm-diameter glass coverslips. Cells were maintained at 37 °C by the use of a closed perfusion chamber [Bioptechs (Butler, PA, U.S.A.) FCS2]. Images were collected using the 100 × -magnification 1.4-numerical aperture Apochromat objective on a Delta Vision–Zeiss restoration microscope. For each cell, 20 optical sections separated by 0.5 μm were recorded, using a Sony Micromax CCD (charge-coupled device) camera and an effective pixel size of 0.265 × 0.265 μm. In all cases the exposure time was 100 ms and the mercury-lamp excitation light was attenuated with a 0.3 neutral-density filter. Three-dimensional images were recorded every 90 s over a period of 15 min for each condition. The three-dimensional motorized stage allowed the imaging of six cells in each experiment. Images were corrected for any fluctuations in mercury-lamp power and restored by iterative constrained deconvolution using an empirically measured point spread

function [20]. Time-lapse images were viewed as single section projections of each time point. All these manipulations were performed using routines contained within the softWoRx image processing package (Applied Precision Inc., Issaquah, WA, U.S.A.).

Immunoelectron microscopy

Cells were cultured on a 10 cm-diameter plastic dishes to 75 % confluency and the medium removed before addition of 8 % (w/v) paraformaldehyde in 0.2 M Pipes, pH 7.2, for 30 min at room temperature, followed by at least 2 days at 4 °C. Cells were then removed from the dish with a plastic cell scraper and pelleted in fixative at approx. 10000 *g* for 30 min. After cryo-protection in 2.1 M sucrose in PBS, ultrathin sections were cut at approx. −100 °C in a Leica ultracryomicrotome and mounted on Pioloform® (polyvinylformal)/carbon-coated grids. Sections were retrieved using the modified pick-up method of Liou et al. [21] and labelled at room temperature as follows. Grids were placed on drops of 0.5 % fish skin gelatin in PBS for 10 min and transferred to drops of rabbit anti-[green fluorescent protein (GFP)] antibody (a gift from Dr David Shima, Endothelial Cell Biology Laboratory, Imperial Cancer Research Fund Laboratories, London, U.K.) for 30 min. Following washes in PBS (3 × 5 min) the grids were incubated on Protein A–gold (8 nm particle size [22]) for 20 min, washed first in PBS (6 × 5 min) and then distilled water (10 × 1 min). The sections were contrasted in methylcellulose/uranyl acetate [23] and observations and photographs taken on a JEOL 1200EX electron microscope. For quantification, micrographs were taken at systematically spaced locations (with a random start) at a primary magnification of 15000 ×. The negatives were scanned at a resolution of 1000 pixels/in ($\approx$ 394 pixels/cm), displayed in Adobe Photoshop 5.5 and square-lattice grids superimposed electronically at a line spacing of 0.5 μm. The length of the plasma membrane and the area of cytoplasm were estimated using principles and formulae described previously [24]. Labelling density of lamellopodia-like protrusions and plasma membrane was compared by systematically scanning immunolabelled cell pellet profiles at a primary magnification of 20000 ×. Intersections of a 'scanning line' defined by a feature on the viewing screen [25] and gold particle labelling observed during scanning were assigned to either lamellopodia or plasma membranes. The estimates of gold density per intersection were calculated as ratio estimates after at least ten scans per pellet profile.

Yeast two-hybrid screen

Myc-tagged human TAPP1 was subcloned into the *Eco*RI/*Sal*I site of pAS2-1 (ClonTech) as a Gal4-DNA-binding domain fusion (GBD). A yeast two-hybrid screen was carried out by co-transforming pAS2-1 TAPP1 and a pACT2 human brain cDNA library fused to the Gal4 activation domain into the yeast strain Y190. The brain library was purchased from ClonTech. Transformed yeast cells were incubated for 10 days at 30 °C on synthetic dropout (SD) agar supplemented with 25 mM 3-aminotriazole and lacking histidine, leucine and tryptophan. Approx. 1 × 10^6 colonies were screened. A total of 140 colonies, which grew on media lacking histidine, leucine and tryptophan, were picked and assayed for expression of the *lacZ* reporter gene, which codes for β-galactosidase. All 140 colonies tested positive in the 5-bromo-4-chloroindol-3-yl β-D-galactopyranoside (X-Gal) assay. The pACT2 plasmids from these clones were isolated and the inserts sequenced using standard procedures in order to identify candidate TAPP1 interacting proteins.
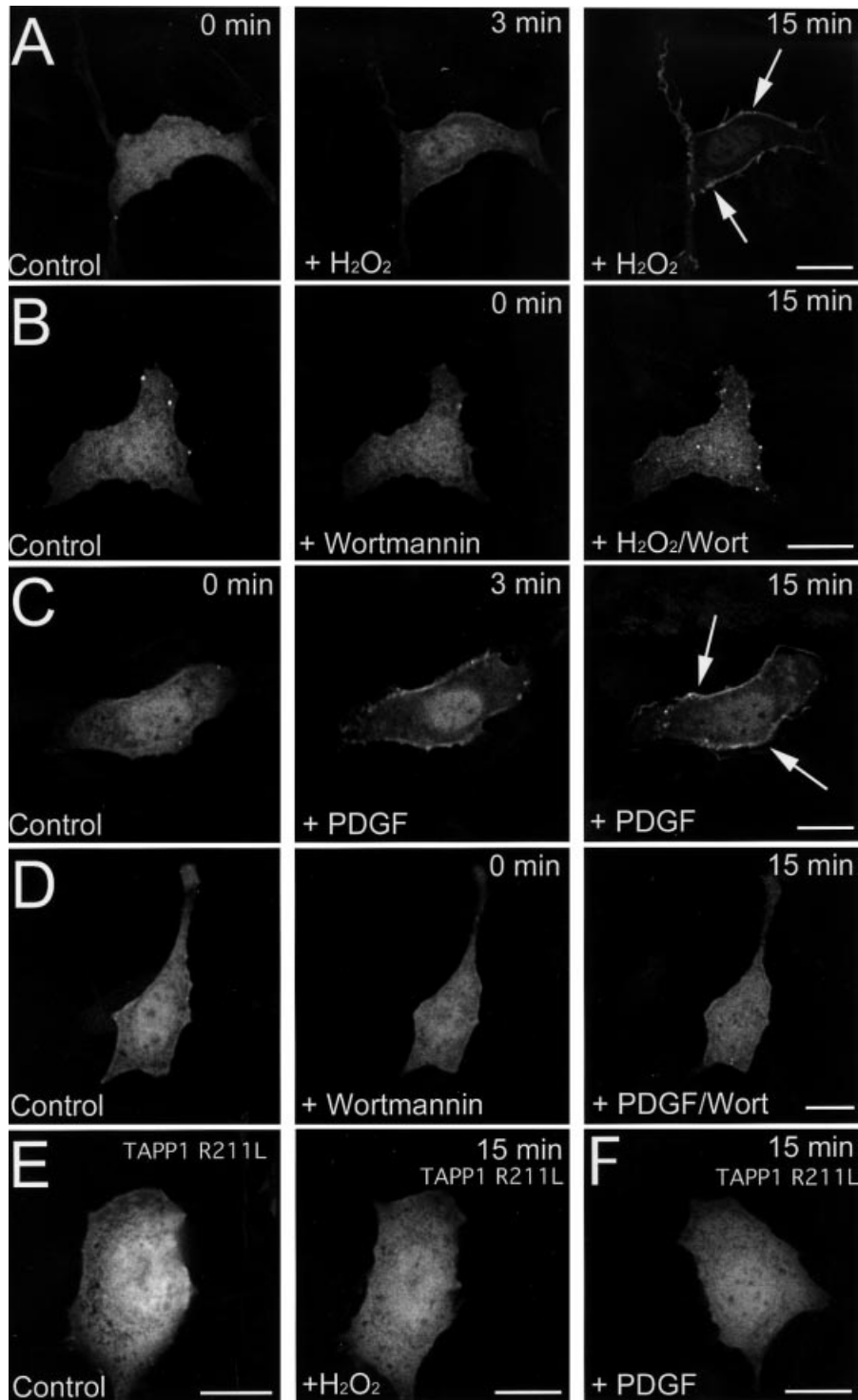
Figure 1   Live-cell imaging of the translocation of YFP–TAPP1$_{CT}$ to the plasma membrane in response to H$_2$O$_2$ and PDGF

Serum-starved Swiss 3T3 cells stably expressing YFP-TAPP1$_{CT}$ were mounted in a heated chamber for live cell fluorescent imaging using a Delta Vision–Zeiss restoration microscope. Images were collected every 90 s. (**A** and **C**) Serum-starved cells were visualized for 15 min, and the panel labelled 'Control' corresponds to the image of the cell after this period. At this point the medium of the cells was exchanged with pre-warmed medium containing either 1 mM H$_2$O$_2$ (**A**) or 50 ng/ml PDGF (**C**) and the cells were observed for a further 15 min, and an image of the cells after 3 and 15 min is shown. (**B** and **D**) As above, except that, after imaging the serum-starved cells for 15 min, the medium of the cells was exchanged with pre-warmed medium containing 100 nM wortmannin and the cells were left incubating with this drug for a further 15 min. The image termed ' + Wortmannin' corresponds to the cells after this period. The medium was then exchanged with pre-warmed medium containing 100 nM wortmannin and either 1 mM H$_2$O$_2$ (**B**) or 50 ng/ml PDGF (**D**) and the cells were observed for a further 15 min. The image of the cell after this period is shown. (**E** and **F**) Serum-starved Swiss 3T3 cells transiently transfected with a construct expressing YFP–TAPP1$_{CT}$[R211L] were either left unstimulated or stimulated with 1 mM H$_2$O$_2$ (**E**) or 50 ng/ml PDGF for 15 min (**F**). For all panels, each experiment was performed at least in duplicate and six separate cells were visualized in each experiment. A representative cell from these experiments is shown. Arrows indicate accumulation of YFP–TAPP1$_{CT}$ at the plasma membrane. The scale bars represent 10 μm. An animated time-lapse version of each panel can be viewed in Movies 1A–1F, which are downloadable from the website given in the text.

Yeast two-hybrid analysis of the interaction of TAPP1/TAPP2 with MUPP1

For the analysis shown in Figure 4 (below), Y190-strain yeasts were co-transformed with the indicated combinations of vectors and grown on SD agar lacking tryptophan and leucine at 30 °C until appearance of colonies. Yeast colonies were picked and resuspended in 50 μl of sterile water and 1 μl dropped on to SD agar lacking leucine and tryptophan or SD agar supplemented with 25 mM 3-aminotriazole and lacking histidine, leucine and tryptophan. The yeast patches were incubated for 2 days at 30 °C and filter lifts taken of yeast grown on SD agar lacking leucine and tryptophan. Reporter β-galactosidase activity of the transformants was tested by incubating filters in X-Gal at 30 °C for 4 h.

Expression of GST–MUPP1 fusion proteins in *E. coli*

The pGEX-2T constructs encoding GST–MUPP1 fragments were transformed into BL21 *E. coli* cells and a 0.5 litre culture was grown at 37 °C in Luria broth containing 100 μg/ml ampicillin, until the A_{600} was 0.6. Isopropyl β-D-galactosidase (250 μM) was added and the cells cultured for a further 16 h at 26 °C. The cells were resuspended in 25 ml of ice-cold Buffer C and lysed by one round of freeze–thawing and the lysates sonicated to fragment the DNA. The lysates were centrifuged at 4 °C for 30 min at 20 000 g, the supernatant filtered through a 0.44 μm-pore-size filter and incubated for 60 min on a rotating platform with 1 ml of GSH–Sepharose previously equilibrated in Buffer C. The suspension was centrifuged for 1 min at 3000 g, the beads washed three times with 15 ml of Buffer C containing 0.5 M NaCl, and then a further ten times with 15 ml of Buffer A. The GSH–Sepharose in an equal volume of Buffer A was divided into aliquots, snap-frozen in liquid nitrogen, and stored at −80 °C. This was employed for the binding assays described in Figure 6 (below).

Binding of wild-type and mutant TAPP1/TAPP2 to MUPP1 fragments in 293 cells

For the results presented in Figure 5 (below), 293 cells were co-transfected with 5 μg of the wild-type or mutant FLAG-epitope-tagged TAPP1/TAPP2 pCMV5 plasmids and 5 μg of the pEBG2T plasmids encoding the indicated GST–MUPP1 C-terminal fragments. At 36 h post-transfection the cells were lysed in 1 ml of Buffer C, the lysates were cleared by centrifugation at 13 000 g for 10 min at 2 °C, and 0.5 mg of supernatant was incubated for 1 h at 4 °C with 5 μl of GSH–Sepharose. The beads were washed twice in Buffer C containing 0.15 M NaCl, followed by two further washes in Buffer A. The beads were resuspended in 20 μl of Sample Buffer and subjected to SDS/PAGE. The gels were analysed by immunoblotting with either anti-FLAG or anti-GST antibodies (described below).

Expression of wild-type and mutant GST–TAPP1 and GST–TAPP2 in human embryonic kidney 293 cells

For purification of GST-fusion proteins, shown in Figure 7(B) below, 10-cm-diameter dishes of 293 cells were transfected with 5 μg of the indicated pEBG-2T construct encoding wild-type or mutant TAPP1 and TAPP2, using a modified calcium phosphate method [26]. At 36 h post-transfection the cells were lysed in 1 ml of Buffer C, the lysates were cleared by centrifugation at 13 000 g for 10 min at 2 °C, and 2 mg of supernatant was incubated for 1 h at 4 °C with 10 μl of GSH–Sepharose. The GST-fusion proteins were purified by affinity chromatography and analysed as described in the legend to Figure 7(B) below.

Immunoprecipitation of endogenous TAPP1 and MUPP1

The polyclonal anti-TAPP1, anti-MUPP1 or anti-LKB1 antibodies (0.5 mg) were covalently coupled to Protein G–Sepharose (0.5 ml) using dimethyl pimelimidate [27]. 293-cell lysates (3 mg) were incubated for 60 min at 4 °C with the Protein G–Sepharose conjugates (15 μl). The immunoprecipitates were washed twice with 1 ml of Buffer C containing 0.15 M NaCl, and washed twice with Buffer B. The beads were resuspended in SDS Sample Buffer that did not contain 2-mercaptoethanol and analysed as described in the legend to Figure 7(A) below.

Immunoblotting

For blots of total cell lysates, 10–20 μg of protein was used. For blots of GST pull-downs or immunoprecipitation, the entire amount of beads was used. Samples were subjected to SDS/PAGE and transferred to nitrocellulose. The membranes were blocked in 50 mM Tris/HCl (pH 7.5/0.15 M NaCl/0.5 % (v/v) Tween (TBS-Tween)/10 % (w/w) skimmed milk for 2 h, then incubated in the same buffer for 7 h at 4 °C in the presence of 1 μg/ml of the indicated primary antibody. Detection was performed using horseradish peroxidase-conjugated secondary antibodies and the enhanced chemiluminescence (ECL®; Amersham Pharmacia Biotech) reagent.

RESULTS

Subcellular localization of the PtdIns(3,4)P_2-binding PH domain of TAPP1

We employed mouse fibroblast Swiss 3T3 cells as a model cell line to investigate whether TAPP1 could interact with PtdIns(3,4)P_2 *in vivo*, since the levels of PtdIns(3,4)P_2 and PtdIns(3,4,5)P_3 generated in response to several stimuli have been well characterized in these cells. For example, stimulation of Swiss 3T3 cells with H_2O_2 (1 mM) induces a > 30-fold elevation in PtdIns(3,4)P_2, whilst only transiently increasing PtdIns(3,4,5)P_3 levels, which returned to basal levels within 15 min. Stimulation with PDGF (50 ng/ml for 10 min), in contrast, induces a moderate increase in PtdIns(3,4)P_2, to ≈ 30 % of the level observed with H_2O_2, but increases basal PtdIns(3,4,5)P_3 levels > 20-fold [14,28]. To perform our analysis, we generated Swiss 3T3 cells that stably express the PtdIns(3,4)P_2-binding PH domain of TAPP1 with an N-terminal YFP tag (YFP–TAPP1$_{CT}$). Fluorescence time-lapse microscopy of living cells revealed that, in unstimulated, Swiss 3T3 cells, YFP–TAPP1$_{CT}$ was diffusely localized in the cytosolic and nuclear compartments. However, stimulation of these cells with H_2O_2 or PDGF induced a rapid recruitment of YFP–TAPP1$_{CT}$ to the plasma membrane, which was apparent within 3 min and TAPP1$_{CT}$ remained located at the membrane for 15 min [Figures 1A and 1C; Movies 1A and 1C (these and subsequently cited animated time-lapse movies are downloadable from http://www.BiochemJ.org/bj/361/bj3610525add.htm)]. Pre-treatment of cells with wortmannin prior to stimulating with H_2O_2 or PDGF prevented the translocation of YFP–TAPP1$_{CT}$ to the plasma membrane (Figures 1B and 1D; Movies 1B and 1D). Similar results were obtained in numerous separate experiments that were performed on unstimulated, H_2O_2- and PDGF-stimulated Swiss 3T3 cells that had been fixed in paraformaldehyde prior to analysing the location of YFP–TAPP1$_{CT}$ by fluorescence microscopy (results not shown). Similar results were also obtained when YFP–TAPP1$_{CT}$ was expressed in Swiss 3T3 cells by transient transfection (results not shown). In Figures 1(E) and 1(F) (and Movies 1E and 1F), we demonstrate that a mutant of TAPP1 that does not interact with PtdIns(3,4)P_2, YFP–TAPP1$_{CT}$[R211L],

was not recruited to the plasma membrane when Swiss 3T3 cells were stimulated with H_2O_2 and PDGF. As a further control we generated Swiss 3T3 cells that stably express YFP alone, which was found to be localized diffusely throughout the cytosol and nucleus in unstimulated, H_2O_2- and PDGF-stimulated cells (results not shown). We also generated human embryonic kidney 293 cells and human glioma U87MG cells, which stably expressed YFP–TAPP1$_{CT}$, and found that exposure of these cells to H_2O_2 induced a very marked translocation of YFP–TAPP1$_{CT}$ to the plasma membrane that was inhibited by wortmannin (results not shown).

Immunogold localization of TAPP1

The subcellular distribution of YFP–TAPP$_{CT}$ was investigated using quantitative immunoelectron microscopy on ultrathin cryosections (Figures 2A–2D). In unstimulated Swiss 3T3 cells there was substantial immunolabelling for YFP–TAPP$_{CT}$ over the cytosol, with little evidence for plasma-membrane localization or localization to intracellular organelles. In contrast, after H_2O_2 and PDGF stimulation, marked labelling of the plasma membrane was observed and, in the case of PDGF, this appeared most concentrated over extended cell protrusions that most likely represented lamellipodia (Figure 2D). This was quantified as described in the Materials and methods section, and it was estimated that there was a 1.9- and 1.7-fold increase in two separate experiments in the labelling concentration in these lamellipodia-like structures derived from PDGF-stimulated cells compared with the rest of the plasma membrane. Further quantitative analysis revealed that, compared with unstimulated cells, H_2O_2 and PDGF produced 10.4- and 5.2-fold overall accumulation of YFP–TAPP$_{CT}$ at the cell surface and also showed that translocation to the plasma membrane was largely prevented by pre-incubation of cells with 100 nM wortmannin prior to stimulation with PDGF and H_2O_2 (Figure 2E).

Evidence that TAPP1 does not interact with PtdIns(3,4,5)P_3 in vivo

We next decided to investigate whether stimulation of Swiss 3T3 cells with an agonist that generated PtdIns(3,4,5)P_3, but only low levels of PtdIns(3,4)P_2, would induce recruitment of YFP–TAPP1$_{CT}$ to the plasma membrane. IGF1 stimulation of Swiss 3T3 cells was shown previously to induce a > 10-fold increase in PtdIns(3,4,5)P_3 over the basal levels, but to only marginally elevate PtdIns(3,4)P_2 [14]. Consistent with TAPP1 only interacting with PtdIns(3,4)P_2, stimulation of Swiss 3T3 cells expressing YFP–TAPP1$_{CT}$ with IGF1 for up to 15 min did not result in a detectable recruitment of TAPP1 to the plasma membrane (Figure 3A; Movie 3A). As a control we showed that IGF1 stimulation of Swiss 3T3 cells induces translocation to the plasma membrane of the YFP-tagged PH domain of GRP1 (Figure 3B; Movie 3B), which binds PtdIns(3,4,5)P_3 but not PtdIns(3,4)P_2 [11,29]. IGF1 also induced recruitment to the plasma membrane of the GFP-tagged PH domain of PKB that binds both PtdIns(3,4,5)P_3 and PtdIns(3,4)P_2 (Figure 3C). IGF1, as expected, failed to induce any movement of the isolated YFP expressed in Swiss 3T3 cells (results not shown).

Interaction of TAPP1 and TAPP2 with MUPP1

In order to identify proteins that interact with TAPP1, we performed a yeast two-hybrid screen in which a human brain library was screened with full-length TAPP1 as the bait. In all, 35 out of the 140 TAPP1-binding 'positive clones' that were characterized corresponded to different C-terminal fragments of
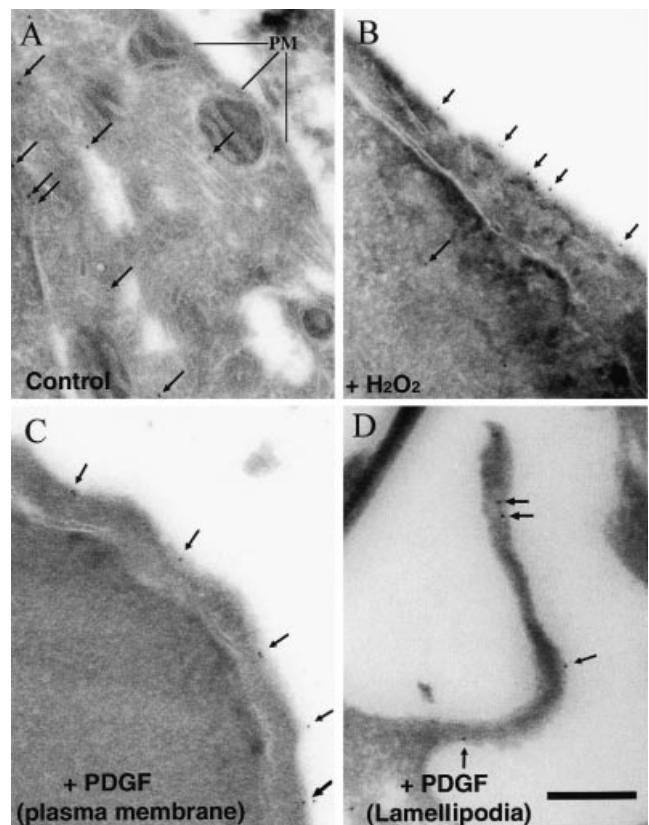
Figure 2   Immunogold localization of YFP–TAPP$_{CT}$

Serum-starved Swiss 3T3 cells stably expressing YFP-TAPP$_{CT}$ were processed for ultrathin cryosectioning and immunolabelled as described in the Materials and methods section. Cells were fixed either untreated (**A**), after 15 min H_2O_2 stimulation (**B**) or after 15 min PDGF stimulation (**C** and **D**). The gold label is indicated by arrows, and in (**A**) the plasma membrane is indicated by 'PM'. The plasma-membrane extension displayed in (**D**) is a lamellipodia structure. The bar represents 250 nm. (**E**) shows the quantitative analysis of immunolabelling of the plasma membrane. Labelled ultrathin cryosections were photographed at systematic random locations and the micrographs analysed using stereological techniques to relate gold labelling to plasma-membrane profile lengths or to the area of cytosol profile (see the Materials and methods section). Results are from a single representative experiment ($n = 7$ for control, $n = 8$ for H_2O_2 and PDGF, $n = 9$ for H_2O_2 + wortmannin and PDGF + wortmannin; error bars represent S.E.M.s of individual ratio estimates).
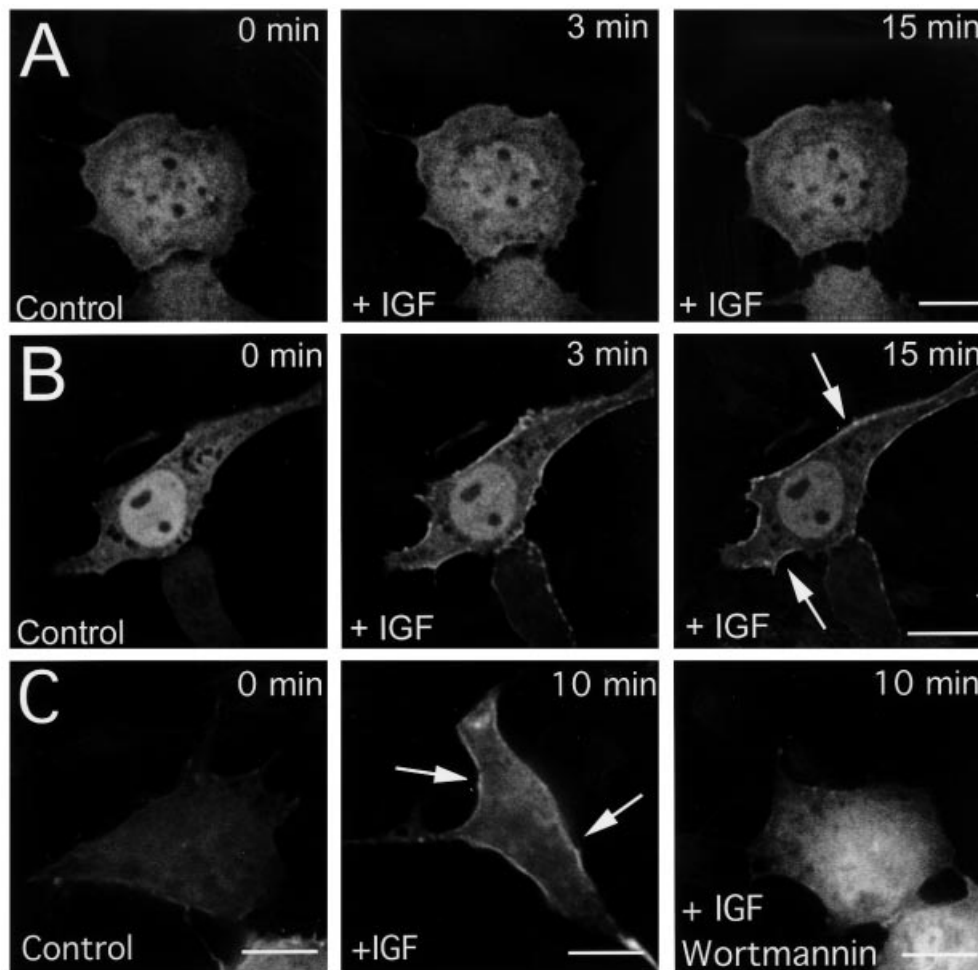
Figure 3   Live-cell imaging of YFP–TAPP1$_{CT}$, YFP–GRP1 and GFP–PKB in unstimulated and IGF1-stimulated Swiss 3T3 cells

Serum-starved Swiss 3T3 cells stably expressing YFP–TAPP1$_{CT}$ were mounted in a heated chamber for live-cell fluorescent imaging using a Delta Vision–Zeiss restoration microscope. Images were collected every 90 s. (**A**) Serum-starved cells were visualized for 15 min and the panel labelled 'Control' corresponds to the image of the cell after this period. At this point the medium was exchanged with pre-warmed medium containing 100 ng/ml IGF1 and the cells were observed for a further 15 min; an image after 3 and 15 min stimulation is shown. (**B**) As above, except that the Swiss 3T3 cells were transiently transfected with a construct expressing the PH domain of YFP–GRP1. At 8 h post-transfection, the cells were serum starved for 16 h prior to imaging. (**C**) Swiss 3T3 cells were transiently transfected with a DNA construct encoding the GFP–PH domain of PKBα and either left unstimulated or stimulated with IGF1 for 10 min in the presence or absence of wortmannin as described above. The cells were fixed with 4% paraformaldehyde and imaged on a Leica microscope as described in the Materials and methods section. For the (**A**) panels, TAPP1$_{CT}$ failed to translocate to the plasma membrane in response to IGF1 in three separate experiments performed on different days. For experiments performed in (**A**) and (**B**), six separate cells were visualized in each experiment. A representative cell from these experiments is shown. Experiments in (**C**) were performed twice with similar results. Arrows indicate accumulation of YFP–GRP1–PH domain and GFP–PKB–PH domain at the plasma membrane. The scale bars represent 10 μM. An animated time-lapse version of each panel can be viewed in Movies 3A and 3B, which are downloadable from the website given in the text.

the 218 kDa multi-PDZ-containing protein termed MUPP1, which possesses 13 sequential PDZ domains and no known catalytic domain. Inspection of the amino acid sequences of TAPP1 and TAPP2 revealed that they are 58% identical over the first 300 amino acids, a region which encompasses both of the PH domains. However, there is no significant similarity between the C-terminal 100 residues of TAPP1 and TAPP2, except that seven out of the 11 extreme C-terminal amino acids of TAPP1 and TAPP2 are identical (Figure 4D). Inspection of the last three residues of TAPP1 and TAPP2 (Ser-Asp-Val), reveal that these conform to the minimal sequence motif required for binding to a PDZ domain ($^{Ser}/_{Thr}$-Xaa-$^{Val}/_{Ile}$ [30,31]). This suggested that TAPP1, as well as TAPP2, might interact through their C-termini with a PDZ domain of MUPP1. The only PDZ domain that was present on all of the MUPP1-interacting clones isolated from the yeast two-hybrid screen was the 13th PDZ domain, indicating that this could be a major site of interaction between

TAPP1 and MUPP1. We therefore initially tested whether wild-type TAPP1, TAPP2 or mutants of TAPP1 and TAPP2 that lack the six C-terminal amino acids (TAPP1ΔCT and TAPP2ΔCT) could interact with a fragment of MUPP1 encompassing only the 13th PDZ domain (MUPP1$_{13}$) or the 11–13th PDZ domain (MUPP1$_{11–13}$). We tested these interactions in a yeast two-hybrid screen (Figure 4) or a mammalian human 293 cell co-expression assay (Figure 5). Both of these assays revealed that wild-type TAPP1 and TAPP2, but not TAPP1ΔCT or TAPP2ΔCT, interacted with MUPP1$_{11–13}$ or MUPP1$_{13}$, confirming that the C-terminal residues of TAPP1 and TAPP2 had the intrinsic ability to interact with at least the 13th PDZ domain of MUPP1. We next tested whether nine fragments of MUPP1 that encompass all 13 PDZ domains were able to bind TAPP1, TAPP1ΔCT, TAPP2 and TAPP2ΔCT (Figure 6). This analysis revealed that fragments of MUPP1 overlapping PDZ domains 1–9 or the isolated 11th or 12th PDZ domain failed to bind to TAPP1 or
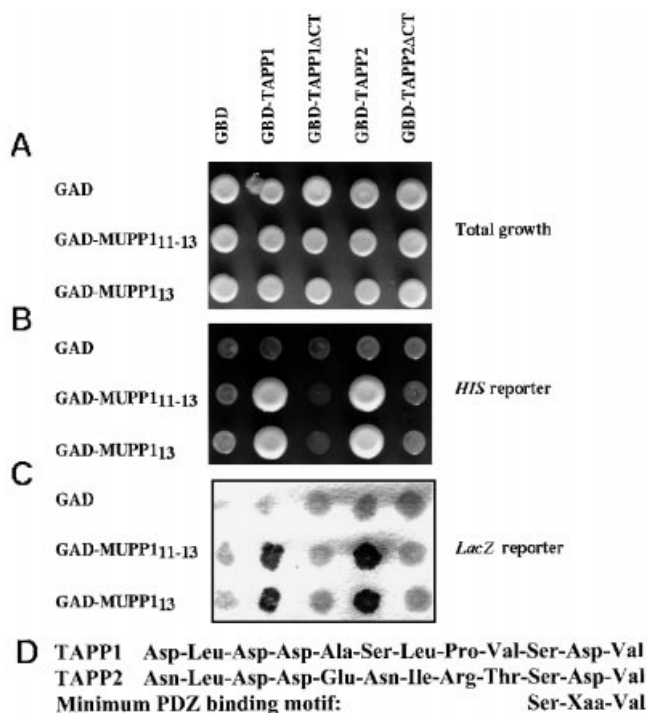
Figure 4   Two-hybrid interaction of TAPP1 and TAPP2 with the C-terminal PDZ domains of MUPP1

Yeast cells were transformed with pACT2 plasmid expressing Gal4 activation domain alone or fused to C-terminal fragments of MUPP1 encompassing the 11–13th PDZ domains (MUPP1$_{11-13}$) or to the isolated 13th PDZ domain of MUPP1 (MUPP1$_{13}$) in the presence of pAS2-1 plasmid coding for the expression of GBD alone or GBD fused to wild-type TAPP1 or TAPP2 or mutants lacking the C-terminal four amino acids (TAPP1$_{CT}$/TAPP2$_{CT}$). In (**A**) yeast cells were grown on SD medium without leucine and tryptophan, in which only those harbouring both pAS2-1 and pACT2 plasmids grow. An interaction between TAPP1/TAPP2 and MUPP1$_{11-13}$/MUPP1$_{13}$ leads to the expression of HIS3 reporter gene, enabling growth on SD medium lacking leucine, tryptophan and histidine, but containing 3-aminotriazole (**B**), and induction of β-galactosidase gene expression (**C**). (**D**) Alignment of the 11 C-terminal amino acid sequence of TAPP1 and TAPP2.

Figure 5   Interaction of TAPP1 and TAPP2 with MUPP1

(**A** and **B**) 293 cells were transiently transfected with DNA constructs coding for the expression of GST, GST–MUPP1$_{11-13}$, GST–MUPP1$_{11-12}$ or GST–MUPP1$_{13}$, together with the indicated wild-type, and mutant forms of FLAG-epitope-tagged TAPP1 and TAPP2. At 36 h post-transfection the cells were lysed and the GST-fusion proteins were purified by affinity chromatography on GSH–Sepharose beads as described in the Materials and methods section. The purified proteins were electrophoresed on an SDS/4–12%-(w/v)-polyacrylamide gel, and immunoblotted using either an anti-FLAG antibody to detect FLAG–TAPP1 or FLAG–TAPP2 or an anti-GST antibody to detect expression of GST-MUPP1 fusion proteins. To establish that the wild-type and mutant TAPP1 and TAPP2 forms were expressed at similar levels, 10 μg of total 293-cell lysate (termed 'total lysate') for each condition were electrophoresed on an SDS/4–12%-polyacrylamide gel and immunoblotted with anti-FLAG antibodies. Similar results were obtained in two different experiments. The positions of the molecular-mass markers (Bio-Rad Precision Markers) are indicated.

TAPP2 significantly. However, the isolated 10th and 13th PDZ domains of MUPP1 interacted significantly with TAPP1 and TAPP2, but not with mutants of these proteins lacking their C-termini (Figure 6).

To investigate whether the interaction of TAPP1 and MUPP1 is physiologically significant, we generated antibodies that could recognize endogenously expressed MUPP1 and TAPP1. We decided to use human 293 cells in the experiments described below, because these cell lines expressed the highest levels of endogenous MUPP1 and TAPP1 among those that we investigated (results not shown). We show in Figure 7 that the immunoprecipitation of endogenous TAPP1 from 293-cell lysates results in the co-immunoprecipitation of endogenous MUPP1. As a control we demonstrated that an antibody that does not immunoprecipitate TAPP1 did not pull down MUPP1. It should be noted that about 10-fold more MUPP1 can be immuno-precipitated from the same amount of cell lysate using a MUPP1 antibody than with a TAPP1 antibody (Figure 7A), indicating that not all of the cellular MUPP1 is associated with TAPP1. However, we cannot exclude the possiblity that some dissociation of the TAPP1–MUPP1 complex occurs during either cell lysis or the immunoprecipitation procedure. We also demonstrate that GST–TAPP1 and GST–TAPP2 expressed in 293 cells and

affinity-purified from cell lysates using GSH–Sepharose is associated with endogenously expressed MUPP1. In contrast, GST–TAPP1ΔCT and GST–TAPP2ΔCT did not interact with endogenous MUPP1 (Figure 7B).

Recruitment of full-length TAPP1 to the plasma membrane requires only the PtdIns(3,4)P_2-binding PH domain

To determine whether the PDZ-binding C-terminus of TAPP1 or its N-terminal PH domain influenced the subcellular localization of TAPP1, 293 cells were transfected with full-length wild-type YFP–TAPP1, YFP–TAPP1ΔCT, TAPP1 possessing a mutation that would disrupt the N-terminal PH domain (YFP–TAPP1[R28L]) or the non-PtdIns(3,4)P_2-binding mutant YFP–TAPP1[R211L]. As observed previously for the isolated C-terminal PtdIns(3,4)P_2-binding PH domain (Figure 1), full-length TAPP1 was localized in the cytosol of unstimulated cells, and H_2O_2 induced its translocation to the plasma membrane, which was prevented by treatment of the cells with wortmannin (Figure 8A). The translocation of full-length TAPP1 to membranes was dependent on the interaction of TAPP1 with PtdIns(3,4)P_2, but not on its PDZ-binding motif, as the YFP–
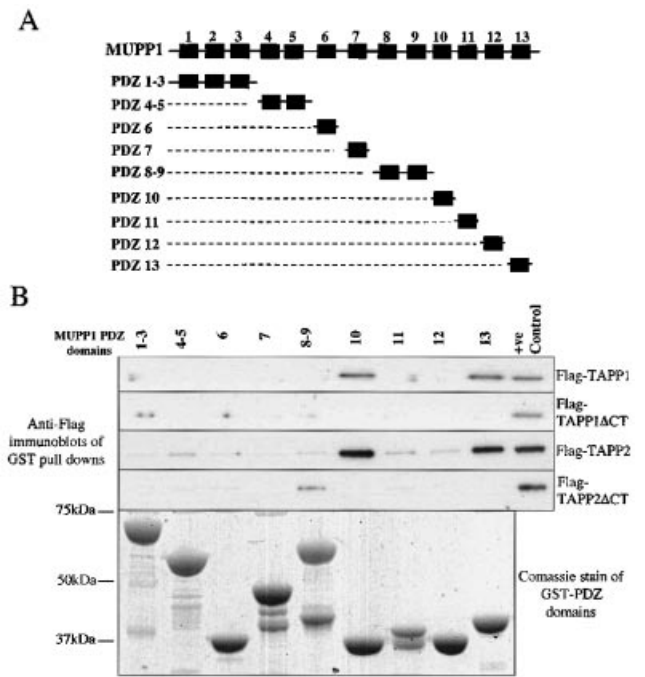
Figure 6   TAPP1 and TAPP2 interact with the 10th and 13th PDZ domains of MUPP1

(**A**) Illustration of the full-length MUPP1 polypeptide and the nine different MUPP1 GST-fusion protein constructs employed. (**B**) A 2 μg portion of the indicated purified GST MUPP1 fusions was electrophoresed on an SDS/4–12%-polyacrylamide gel and stained with Coomassie Brilliant Blue. The positions of the molecular-mass markers (Bio-Rad Precision Markers) are indicated. The indicated GST–MUPP1 fusion proteins (5 μg) bound to GSH–Sepharose (5 μl) were incubated for 1 h in 293-cell lysates (0.2 mg) expressing the FLAG-epitope-tagged TAPP1 or TAPP1ΔCT or TAPP2 or TAPP2ΔCT. The GSH–Sepharose–MUPP1 complexes were isolated and washed as described in the Materials and methods section. These were then electrophoresed on a 4–12% (w/v)-polyacrylamide gel and immunoblotted with a FLAG antibody to detect the presence of TAPP1- or TAPP2-associated with GST–MUPP1 fusion proteins. Identical results were obtained in two separate experiments.

TAPP1[R211L] mutant remained in the cytosol (Figure 8C), whereas the mutant YFP–TAPP1ΔCT was recruited to the plasma membrane in response to H_2O_2 (Figure 8D). We reported previously that the N-terminal PH domain of TAPP1 does not bind PtdIns(3,4,5)P_3 or PtdIns(3,4)P_2 or any other phospho-inositide that was tested [32]. Consistent with this observation, the N-terminal PH domain mutant of TAPP1, YFP–TAPP1[R28L] is recruited to cell membranes by H_2O_2 as effectively as wild-type TAPP1 (Figure 8B).

DISCUSSION

The present results indicate that PtdIns(3,4)P_2 is likely to be a physiological ligand for the C-terminal PH domain of TAPP1. This is based on the finding that stimulation of Swiss 3T3 cells with H_2O_2 or PDGF (Figures 1 and 2), 293 cells with H_2O_2 (Figure 8) and U87MG cells with H_2O_2 (results not shown), induces the marked translocation of TAPP1 to the plasma membrane, where PtdIns(3,4)P_2 would be expected to be located (see below). Consistent with translocation of TAPP1 to the plasma membrane being mediated through its interaction with PtdIns(3,4)P_2, it is prevented by wortmannin, a compound that inhibits PtdIns(3,4)P_2 production, or by mutation of a conserved arginine residue that is required for the interaction of TAPP1 with PtdIns(3,4)P_2 (Figures 1, 2 and 8). In contrast, stimulation
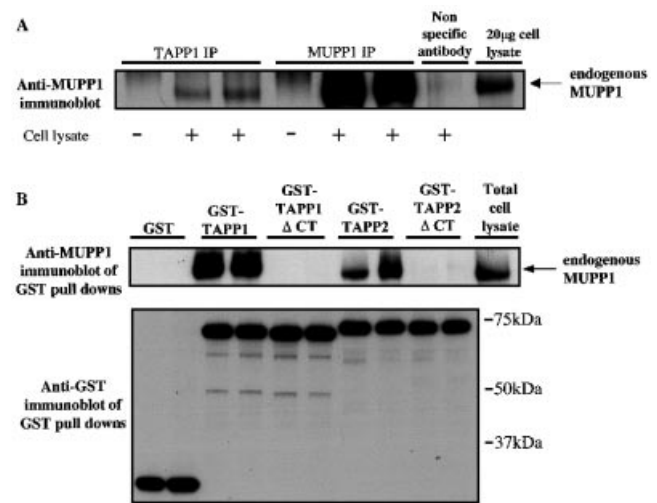
Figure 7   Interaction of endogenous TAPP1 with endogenous MUPP1

(**A**) Antibodies recognizing TAPP1, MUPP1 and a protein kinase termed LKB1 (non-specific antibody) were covalently coupled to Protein G–Sepharose and were incubated in the presence (+) or absence (−) of 293-cell lysate (5 mg) for 2 h, and the immunoprecipitates were washed as described in the Materials and methods section. The washed immunoprecipitates were electrophoresed on a 3–8%-(w/v)-polyacrylamide gel together with 20 μg of total 293-cell lysate and immunoblotted with an anti-MUPP1 antibody. (**B**) 293 cells were transiently transfected with DNA constructs expressing wild-type GST–TAPP1, GST–TAPP2 or mutant GST–TAPP1-ΔCT and TAPP2-ΔCT. At 36 h post-transfection the cells were lysed and the GST-fusion proteins purified by affinity chromatography on GSH–Sepharose beads. The purified proteins were electrophoresed on a 3–8%-(w/v)-polyacrylamide gel and immunoblotted with either an anti-MUPP1 antibody to detect the presence of endogenous MUPP1 or an anti-GST antibody to detect expression of wild-type and mutant GST–TAPP1 and GST–TAPP2. The positions of the molecular-mass markers (Bio-Rad Precision Markers) are indicated.

of Swiss 3T3 cells with IGF1, an agonist that elevates PtdIns(3,4,5)P_3 without markedly increasing PtdIns(3,4)P_2, induced the translocation to the plasma membrane of the GRP1 PH domain that binds PtdIns(3,4,5)P_3 specifically or the PH domain of PKB that binds both PtdIns(3,4,5)P_3 and PtdIns(3,4)P_2, but failed to recruit TAPP1$_{CT}$ (Figure 3). If Ins(1,3,4)P_3 or Ins(1,3,4,5)P_4 were physiological ligands for TAPP1, one would expect TAPP1 not to translocate to the plasma membrane in response to H_2O_2 or PDGF, as these inositol phosphate species would not be expected to be located at the plasma membrane. We also expressed two mutants of TAPP1, YFP–TAPP1[A203G,V204G] and YFP–TAPP1[A203G], which interact with both PtdIns-(3,4)P_2 and PtdIns(3,4,5)P_3 *in vitro* [16], in Swiss 3T3 cells in order to verify whether IGF1 stimulation of these cells induced translocation of this mutant to the plasma membrane. Unfortunately, in numerous experiments, IGF1 did not induce a translocation of these mutants to the plasma membrane (results not shown). Even H_2O_2 only poorly induced the recruitment of these mutants of TAPP1 to the plasma membrane, indicating that they interact poorly with PtdIns(3,4)P_2 *in vivo*. The reasons for this are unclear, but, because of this finding, we cannot definitively rule out the possibility that TAPP1 may also interact very weakly with PtdIns(3,4,5)P_3 *in vivo* and that IGF1 stimulation does not produce sufficient amounts of PtdIns(3,4,5)P_3 to recruit TAPP1 to the membrane.

The cellular location of PtdIns(3,4,5)P_3 has been studied extensively in numerous cell lines using GFP-tagged PH domains which interact specifically with PtdIns(3,4,5)P_3, such as GRP1 [28,33,34] or Bruton's tyrosine kinase (BTK) [35]. These investigations have established that GFP–GRP1 and GFP–BTK PH
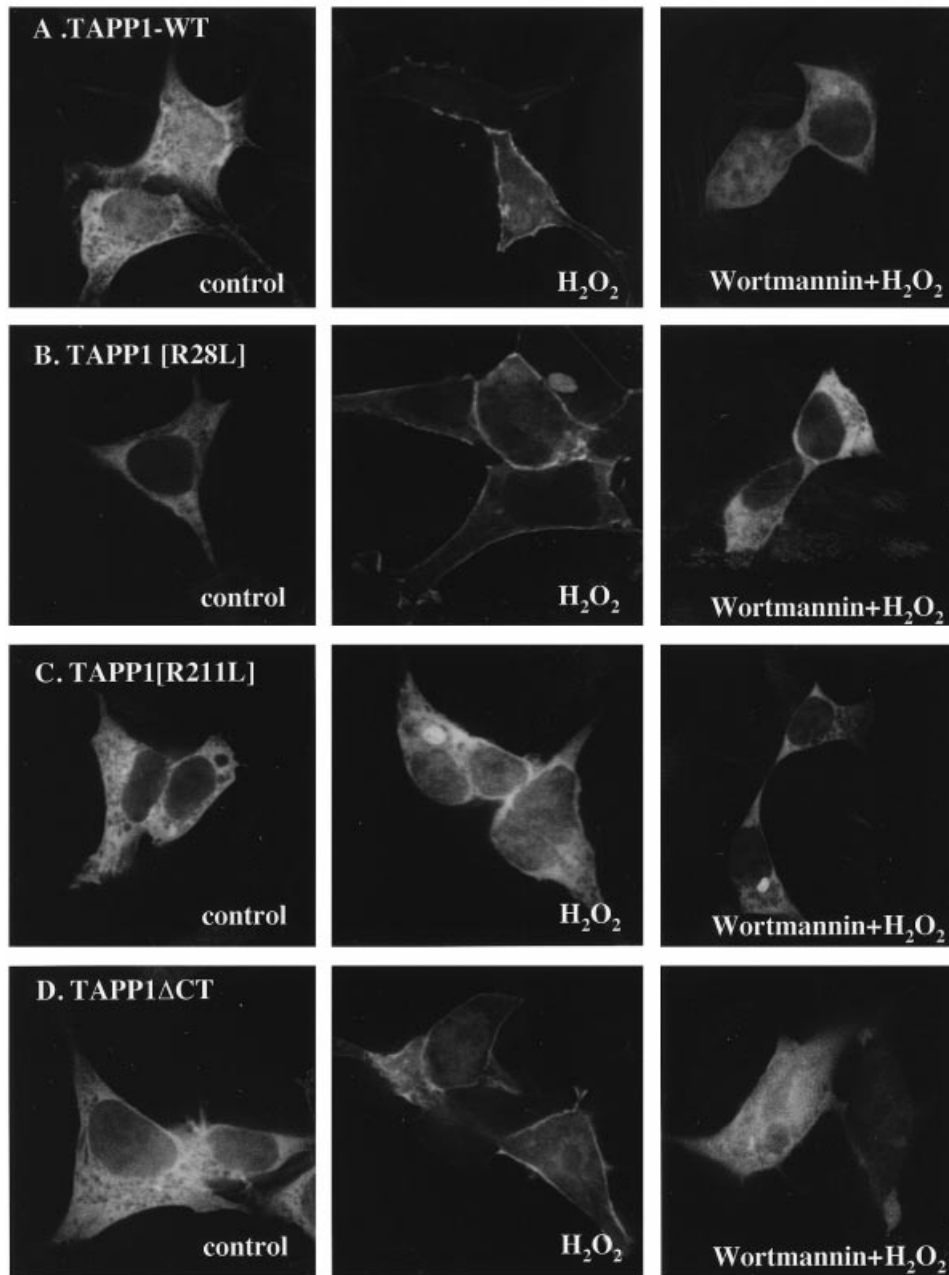
Figure 8   Localization of full-length wild-type and mutant TAPP1 in unstimulated and H$_2$O$_2$-stimulated cells

293 cells were transiently transfected with DNA constructs encoding for the expression of wild-type and indicated mutants of TAPP1. At 16 h post-transfection the cells were serum-starved and either left unstimulated or stimulated with 1 mM H$_2$O$_2$ for 15 min or treated with 100 nM wortmannin for 10 min and then stimulated with H$_2$O$_2$ for 15 min. The cells were then fixed in 4% (w/v) paraformaldehyde and imaged using a Leica microscope as described in the Materials and methods section. The cells shown are representative images obtained in two separate experiments.

domains are recruited to the plasma membrane, in response to insulin, growth factors and other agonists that activate PI 3-kinases. This indicates that the bulk of cellular PtdIns(3,4,5)P_3 is localized at the plasma membrane. Our results validate the use of the C-terminal PH domain of TAPP1 as a probe to monitor the intracellular formation and location of PtdIns(3,4)P_2 selectively. In a previous study, the PH domain of PKB, which binds both PtdIns(3,4,5)P_3 and PtdIns(3,4)P_2 was used to suggest that PtdIns(3,4)P_2 was located at the plasma membrane in H$_2$O$_2$-stimulated cells [28]. However, in this experiment it is not

possible to exclude the possiblity that at least some of the membrane localization observed was caused by the interaction of PKB with PtdIns(3,4,5)P_3 rather than PtdIns(3,4)P_2 [28]. The only other protein that has been reported to interact with PtdIns(3,4)P_2 *in vitro* with some selectivity over other phosphoinositides is the PX domain of the p47^{phox} subunit of the phagocytic NADPH oxidase complex [36]. However, it is unlikely that interaction of the p47^{phox} PX domain with PtdIns(3,4)P_2 is a sufficiently specific probe for PtdIns(3,4)P_2 formation *in vivo*, because it also interacts with PtdIns(3,4,5)P_3, PtdIns(3,5)P_2 and

PtdIns$3P$, with only marginally lower affinity than it bound to PtdIns(3,4)P_2 [36].

Our observations indicate that the bulk of PtdIns(3,4)P_2 generated in response to H_2O_2 and PDGF is located at the plasma membrane. The PtdIns(3,4)P_2 formed in response to PDGF is likely to be generated through the dephosphorylation of PtdIns(3,4,5)P_3 by the 5-phosphatases SHIP1/SHIP2 [37,38]. As PtdIns(3,4,5)P_3 is located at the plasma membrane and the SHIP1/SHIP2 phosphatases are also recruited to the plasma membrane following stimulation of cells with growth factors [5], this would account for the plasma-membrane localization of PtdIns(3,4)P_2 following PDGF stimulation. In contrast, the pathway by which H_2O_2 can increase cellular levels of PtdIns-(3,4)P_2 is not known. However, one possibility is that H_2O_2 activates PI 3-kinase by inhibiting tyrosine phosphatases [14], and also inhibits PTEN (phosphatase and tensin homologue deleted on chromosome 10), the major PtdIns(3,4,5)P_3 3-phosphatase, but not SHIP2 (D. Bennett and C. P. Downes, unpublished work). If this were the case, we favour the view that PtdIns(3,4)P_2 could be generated in response to H_2O_2 through the dephosphorylation of PtdIns(3,4,5)P_3. This would be consistent with the finding that H_2O_2 recruits TAPP1 to the plasma membrane. However, PtdIns(3,4)P_2 may not always be localized at the plasma membrane. As described in the Introduction, in platelets, PtdIns(3,4)P_2 can also be generated through the phosphorylation of PtdIns$3P$ by an as-yet-uncharacterised PI 4-kinase [13]. As the bulk of cellular PtdIns$3P$ is endosomal [39], it is possible that PtdIns(3,4)P_2 generated through the phosphorylation of PtdIns$3P$ is located at the endosomes or other intracellular compartment rather than at the plasma membrane. It will therefore be important in future studies to exploit the ability of TAPP1 or TAPP2 to bind PtdIns(3,4)P_2, to investigate the location of PtdIns(3,4)P_2 in fibrinogen-stimulated platelets [12] or in other cells where PtdIns(3,4)P_2 is produced by the phosphorylation of PtdIns$3P$. It should be noted that Fukui and colleagues [40] have generated a monoclonal antibody that apparently recognized PtdIns(3,4)P_2 specifically and demonstrated that following H_2O_2 stimulation of 293 cells, PtdIns-(3,4)P_2 is localized both at the plasma membrane and at the nuclear membrane. This latter observation contrasts with our findings using TAPP1 as a probe of PtdIns(3,4)P_2, in which we see no evidence of recruitement of TAPP1 to the nuclear membrane in H_2O_2-stimulated Swiss 3T3 and 293 cells (Figures 1, 2 and 8).

We identified MUPP1 as a protein that can interact with both TAPP1 and TAPP2 and provide evidence that the endogenously expressed TAPP1 forms a complex with MUPP1. We also demonstrated that the 10th and 13th PDZ domains of MUPP1 can interact with wild-type TAPP1 and TAPP2, but not with mutants that lack the C-terminal four amino acids. Little is known about the physiological roles of MUPP1. Recently, it has been shown that two oncoproteins termed E4-ORF1 and E6 that are encoded by the DNA viruses adenovirus type 9 and high-risk human papillomavirus respectively interact with MUPP1. Expression of E4-ORF1 or E6 in cells promotes proliferation, and this has been shown to be dependent on their ability to interact with MUPP1 [19] and perhaps other PDZ-domain-containing proteins [41]. Interestingly, E4-ORF1 binds to both the 7th and 10th PDZ domain of MUPP1 and sequesters MUPP1 within the cytoplasm of cells, whereas the interaction of E6 with MUPP1 induces its degradation [19]. These results imply that MUPP1 may negatively regulate cellular proliferation and may need to be located at the plasma membrane of cells to inhibit cell growth. It could be speculated that the binding of TAPP1 and TAPP2 to MUPP1 recruits MUPP1 (and other proteins that

it is associated with) to the plasma membrane in response to agonists that elevate PtdIns(3,4)P_2. This may play a role in suppressing cell growth.

Three other proteins have also been shown to interact with the 10th PDZ domain of MUPP1, namely the 5-hydroxytryptamine type 2C receptor [42], the c-Kit tyrosine kinase [43] and the tight-junction protein claudin-1 [44]. We have aligned the C-termini of these proteins, but, apart from a C-terminal valine residue, there are no other conserved residues that could explain why these proteins interact with the 10th PDZ domain of MUPP1. However, unlike TAPP1 and TAPP2, the 5-hydroxytryptamine type 2C receptor, the c-Kit tyrosine kinase and claudin-1 do not interact with the 13th PDZ domain of MUPP1 [42,43].

In summary, we provide evidence that PtdIns(3,4)P_2 and MUPP1 are physiological ligands for TAPP1 and TAPP2. This indicates that TAPP1 and TAPP2 may regulate physiological processes that are controlled by PtdIns(3,4)P_2 and could function as adaptor proteins to recruit TAPP1/TAPP2-binding proteins, such as MUPP1, to membranes in response to agonists that induce the production of PtdIns(3,4)P_2. To define the roles that TAPP1 and or TAPP2 play in cells, it will not only be important to identify the proteins with which they interact, but to knock out TAPP1 and TAPP2 in mice and/or cells and determine how this affects processes that are known to be regulated by growth factors and other stimuli that increase PtdIns(3,4)P_2.

REFERENCES

1 Vanhaesebroeck, B., Leevers, S. J., Ahmadi, K., Timms, J., Katso, R., Driscoll, P. C., Woscholski, R., Parker, P. J. and Waterfield, M. D. (2001) Synthesis and Function of 3-phosphorylated inositol lipids. Annu. Rev. Biochem. **70**, 535–602

2 Lemmon, M. A. and Ferguson, K. M. (2000) Signal-dependent membrane targeting by pleckstrin homology (PH) domains. Biochem. J. **350**, 1–18

3 Vanhaesebroeck, B. and Alessi, D. R. (2000) The PI3K–PDK1 connection: more than just a road to PKB. Biochem. J. **346**, 561–576

4 Leslie, N. R., Biondi, R. M. and Alessi, D. R. (2001) Phosphoinositide-regulated kinases and phosphoinositde phosphatases. Chem. Rev. **101**, 2365–2380

5 Pesesse, X., Dewaste, V., De Smedt, F., Laffargue, M., Giuriato, S., Moreau, C., Payrastre, B. and Erneux, C. (2001) The src homology 2 domain containing inositol 5-phosphatase SHIP2 is recruited to the epidermal growth factor (EGF) receptor and dephosphorylates phosphatidylinositol 3,4,5-trisphosphate in EGF-stimulated cos-7 cells. J. Biol. Chem. **276**, 28348–28355

6 James, S. R., Downes, C. P., Gigg, R., Grove, S. J., Holmes, A. B. and Alessi, D. R. (1996) Specific binding of the Akt-1 protein kinase to phosphatidylinositol 3,4,5-trisphosphate without subsequent activation. Biochem. J. **315**, 709–713

7 Stephens, L., Anderson, K., Stokoe, D., Erdjument-Bromage, H., Painter, G. F., Holmes, A. B., Gaffney, P. R., Reese, C. B., McCormick, F., Tempst, P. et al. (1998) Protein kinase B kinases that mediate phosphatidylinositol 3,4,5-trisphosphate-dependent activation of protein kinase B. Science **279**, 710–714

8 Walker, K. S., Deak, M., Paterson, A., Hudson, K., Cohen, P. and Alessi, D. R. (1998) Activation of protein kinase B β and γ isoforms by insulin *in vivo* and by 3-phosphoinositide-dependent protein kinase-1 *in vitro*: comparison with protein kinase Bα. Biochem. J. **331**, 299–308

9   Anderson, K. E., Lipp, P., Bootman, M., Ridley, S. H., Coadwell, J., Ronnstrand, L., Lennartsson, J., Holmes, A. B., Painter, G. F., Thuring, J. et al. (2000) DAPP1 undergoes a PI 3-kinase-dependent cycle of plasma-membrane recruitment and endocytosis upon cell stimulation. Curr. Biol. **10**, 1403–1412

10 Dowler, S., Currie, R. A., Downes, C. P. and Alessi, D. R. (1999) DAPP1: a dual adaptor for phosphotyrosine and 3-phosphoinositides. Biochem. J. **342**, 7–12

11 Ferguson, K. M., Kavran, J. M., Sankaran, V. G., Fournier, E., Isakoff, S. J., Skolnik, E. Y. and Lemmon, M. A. (2000) Structural basis for discrimination of 3-phosphoinositides by pleckstrin homology domains. Mol. Cell. **6**, 373–384

12 Banfic, H., Downes, C. P. and Rittenhouse, S. E. (1998) Biphasic activation of PKBα/Akt in platelets. Evidence for stimulation both by phosphatidylinositol 3,4-bisphosphate, produced via a novel pathway, and by phosphatidylinositol 3,4,5-trisphosphate. J. Biol. Chem. **273**, 11630–11637

13 Banfic, H., Tang, X., Batty, I. H., Downes, C. P., Chen, C. and Rittenhouse, S. E. (1998) A novel integrin-activated pathway forms PKB/Akt-stimulatory phosphatidylinositol 3,4-bisphosphate via phosphatidylinositol 3-phosphate in platelets. J. Biol. Chem. **273**, 13–16

14 Van der Kaay, J., Beck, M., Gray, A. and Downes, C. P. (1999) Distinct phosphatidylinositol 3-kinase lipid products accumulate upon oxidative and osmotic stress and lead to different cellular responses. J. Biol. Chem. **274**, 35963–35968

15 Dowler, S., Currie, R. A., Campbell, D. G., Deak, M., Kular, G., Downes, C. P. and Alessi, D. R. (2000) Identification of pleckstrin-homology-domain-containing proteins with novel phosphoinositide-binding specificities. Biochem. J. **351**, 19–31

16 Thomas, C. C., Dowler, S., Deak, M., Alessi, D. R. and Van Aalten, D. M. (2001) Crystal structure of the phosphatidylinositol 3,4-bisphosphate-binding pleckstrin homology (PH) domain of tandem PH-domain-containing protein 1 (TAPP1): molecular basis of lipid specificity. Biochem. J. **358**, 287–294

17 Ullmer, C., Schmuck, K., Figge, A. and Lubbert, H. (1998) Cloning and characterization of MUPP1, a novel PDZ domain protein. FEBS Lett. **424**, 63–68

18 Sapkota, G. P., Kieloch, A., Lizcano, J. M., Lain, S., Arthur, J. S., Williams, M. R., Morrice, N., Deak, M. and Alessi, D. R. (2001) Phosphorylation of the protein kinase mutated in Peutz–Jeghers cancer syndrome, LKB1/STK11, at Ser431 by p90RSK and cAMP-dependent protein kinase, but not its farnesylation at Cys433, is essential for LKB1 to suppress cell growth. J. Biol. Chem. **276**, 19469–19482

19 Lee, S. S., Glaunsinger, B., Mantovani, F., Banks, L. and Javier, R. T. (2000) Multi-PDZ domain protein MUPP1 is a cellular target for both adenovirus E4-ORF1 and high-risk papillomavirus type 18 E6 oncoproteins. J. Virol. **74**, 9680–9693

20 Agard, D. A., Hiraoka, Y., Shaw, P. and Sedat, J. W. (1989) Fluorescence microscopy in three dimensions. Methods Cell. Biol. **30**, 353–377

21 Liou, W., Geuze, H. J. and Slot, J. W. (1996) Improving structural integrity of cryosections for immunogold labeling. Histochem. Cell Biol. **106**, 41–58

22 Lucocq, J. M. (1993) Particulate markers for immunoelectron microscopy. In Fine Structure Immunocytochemistry (Griffiths, G., ed.), pp. 279–302, Springer-Verlag, Berlin

23 Griffiths, G., McDowall, A., Back, R. and Dubochet, J. (1984) On the preparation of cryosections for immunocytochemistry. J. Ultrastruct. Res. **89**, 65–78

24 Lucocq, J. (1994) Quantitation of gold labelling and antigens in immunolabelled ultrathin sections. J. Anat. **184**, 1–13

25 Lucocq, J. M. (2001). Electron microscopy in cell biology. In Essential Cell Biology, A Practical Approach (Davey, J. A., Lord, M., eds.), Oxford University Press, Oxford, in the press

26 Alessi, D. R., Andjelkovic, M., Caudwell, B., Cron, P., Morrice, N., Cohen, P. and Hemmings, B. A. (1996) Mechanism of activation of protein kinase B by insulin and IGF-1. EMBO J. **15**, 6541–6551

27 Harlow, E. and Lane, D. (1988) Antibodies: a Laboratory Manual, Cold Spring Harbor Laboratory Press, Cold Spring Harbor, NY

28 Gray, A., Van Der Kaay, J. and Downes, C. P. (1999) The pleckstrin homology domains of protein kinase B and GRP1 (general receptor for phosphoinositides-1) are sensitive and selective probes for the cellular detection of phosphatidylinositol 3,4-bisphosphate and/or phosphatidylinositol 3,4,5-trisphosphate in vivo. Biochem. J. **344**, 929–936

29 Lietzke, S. E., Bose, S., Cronin, T., Klarlund, J., Chawla, A., Czech, M. P. and Lambright, D. G. (2000) Structural basis of 3-phosphoinositide recognition by pleckstrin homology domains. Mol. Cell. **6**, 385–394

30 Kornau, H. C., Schenker, L. T., Kennedy, M. B. and Seeburg, P. H. (1995) Domain interaction between NMDA receptor subunits and the postsynaptic density protein PSD-95. Science **269**, 1737–1740

31 Songyang, Z., Fanning, A. S., Fu, C., Xu, J., Marfatia, S. M., Chishti, A. H., Crompton, A., Chan, A. C., Anderson, J. M. and Cantley, L. C. (1997) Recognition of unique carboxyl-terminal motifs by distinct PDZ domains. Science **275**, 73–77

32 Dowler, S., Montalvo, L., Cantrell, D., Morrice, N. and Alessi, D. R. (2000) Phosphoinositide 3-kinase-dependent phosphorylation of the dual adaptor for phosphotyrosine and 3-phosphoinositides by the Src family of tyrosine kinase. Biochem. J. **349**, 605–610

33 Venkateswarlu, K., Gunn-Moore, F., Oatey, P. B., Tavare, J. M. and Cullen, P. J. (1998) Nerve growth factor- and epidermal growth factor-stimulated translocation of the ADP-ribosylation factor-exchange factor GRP1 to the plasma membrane of PC12 cells requires activation of phosphatidylinositol 3-kinase and the GRP1 pleckstrin homology domain. Biochem. J. **335**, 139–146

34 Klarlund, J. K., Guilherme, A., Holik, J. J., Virbasius, J. V., Chawla, A. and Czech, M. P. (1997) Signaling by phosphoinositide-3,4,5-trisphosphate through proteins containing pleckstrin and Sec7 homology domains. Science **275**, 1927–1930

35 Varnai, P., Rother, K. I. and Balla, T. (1999) Phosphatidylinositol 3-kinase-dependent membrane association of the Bruton's tyrosine kinase pleckstrin homology domain visualized in single living cells. J. Biol. Chem. **274**, 10983–10989

36 Kanai, F., Liu, H., Field, S. J., Akbary, H., Matsuo, T., Brown, G. E., Cantley, L. C. and Yaffe, M. B. (2001) The PX domains of p47phox and p40phox bind to lipid products of PI(3)K. Nat. Cell. Biol. **3**, 675–678

37 Liu, Q., Sasaki, T., Kozieradzki, I., Wakeham, A., Itie, A., Dumont, D. J. and Penninger, J. M. (1999) SHIP is a negative regulator of growth factor receptor-mediated PKB/Akt activation and myeloid cell survival. Genes Dev. **13**, 786–791

38 Clement, S., Krause, U., Desmedt, F., Tanti, J. F., Behrends, J., Pesesse, X., Sasaki, T., Penninger, J., Doherty, M., Malaisse, W. et al. (2001) The lipid phosphatase SHIP2 controls insulin sensitivity. Nature (London) **409**, 92–97

39 Stenmark, H. and Aasland, R. (1999) FYVE-finger proteins – effectors of an inositol lipid. J. Cell Sci. **112**, 4175–4183

40 Yokogawa, T., Nagata, S., Nishio, Y., Tsutsumi, T., Ihara, S., Shirai, R., Morita, K., Umeda, M., Shirai, Y., Saitoh, N. and Fukui, Y. (2000) Evidence that 3′-phosphorylated polyphosphoinositides are generated at the nuclear surface: use of immunostaining technique with monoclonal antibodies specific for PI 3,4-P_2. FEBS Lett **473**, 222–226

41 Glaunsinger, B. A., Lee, S. S., Thomas, M., Banks, L. and Javier, R. (2000) Interactions of the PDZ-protein MAGI-1 with adenovirus E4-ORF1 and high-risk papillomavirus E6 oncoproteins. Oncogene **19**, 5270–5280

42 Becamel, C., Figge, A., Poliak, S., Dumuis, A., Peles, E., Bockaert, J., Lubbert, H. and Ullmer, C. (2001) Interaction of serotonin 5-hydroxytryptamine type 2C receptors with PDZ10 of the multi-PDZ domain protein MUPP1. J. Biol. Chem. **276**, 12974–12982

43 Mancini, A., Koch, A., Stefan, M., Niemann, H. and Tamura, T. (2000) The direct association of the multiple PDZ domain containing protein MUPP-1 with the human c-Kit C-terminus is regulated by tyrosine kinase activity. FEBS Lett. **482**, 54–58

44 Hamazaki, Y., Itoh, M., Sasaki, H., Furuse, M. and Tsukita, S. (2001) Multi-PDZ-containing protein 1 (MUPP1) is concentrated at tight junctions through its possible interaction with claudin-1 and junctional adhesion molecule (JAM). J. Biol. Chem., in the press